Progress In Electromagnetics Research Letters, Vol. 85, 25–30, 2019

Monthly Cloud Free LOS Time Series Generator for Optical Satellite Links

Nikolaos K. Lyras, Theodore T. Kapsis, and Athanasios D. Panagopoulos*

Abstract—In this Letter, a space time synthesizer for the generation of monthly cloud free line of sight (CFLOS) statistics is presented. The proposed monthly time series generator is based on the synthesis of 3D cloud fields using Stochastic Differential Equations. Monthly Integrated Liquid Water Content (ILWC) statistics are used as inputs, and the temporal and spatial correlation of clouds is considered. The monthly variability of the cloud coverage is predicted, and the CFLOS is estimated taking into account the elevation angle of the slant path and the altitude of the station for high altitude optical ground stations. Finally, CFLOS numerical results are reported, and some significant conclusions are drawn.

1. INTRODUCTION

Nowadays, there is increasing interest for broadband internet and interactive satellite services. Additionally in a few years the amount of data that each user produces and transmits will be dramatically increased. To meet these demands, the new designed high throughput satellite systems are shifting to higher frequency bands. On one hand, there is the RF solution of shifting to Q/V or even W bands, and on the other hand, a prominent solution is the use of optical frequencies for GEO Satellite. Compared to RF satellite systems, FSO technology has a great variety of advantages such as the capability for higher throughput, reduced mass, low energy consumption, improved security no interception, and there is no need of regulation up to now, among others [1].

Free Space Optical (FSO) satellite communication systems are severely affected by atmospheric phenomena [1]. Among the phenomena that impair the link, clouds constitute the dominant restricted factor since clouds cause the blockage of the optical link. To overcome cloud coverage site diversity technique is used [1]. In this technique, multiple interconnected optical ground stations (OGSs) forming an OGS network (OGSN) are employed to increase the availability of the whole network. If at least one OGS is not blocked by clouds, then the OGSN is assumed free of clouds. For the design of FSO satellite communication systems Cloud-Free Line of Sight (CFLOS) probability should be accurately predicted for both single links but also for multiple OGSs taking into account the spatial and temporal correlation of clouds among others. In [2–4] single and joint CFLOS probabilities are estimated using cloud mask data and in [5–7] using ILWC statistics taking into account the spatial and temporal variability of clouds among others.

The usage of monthly statistics in the design of optical satellite communication systems may be proved of prominent importance since cloud coverage displays significant monthly variations. For example, in the following Fig. 1(a), the mean monthly probability of cloud coverage for each month in three locations Catania, Italy; Mallorca, Spain; and Suez, Egypt for the years from 2012 up to 2015 as derived from ERA Interim are reported. It must be noticed that the mean annual values for the same period for Catania is 0.2785, Mallorca 0.306, and Suez is 0.1971.

Received 21 December 2018, Accepted 1 June 2019, Scheduled 13 June 2019
* Corresponding author: Athanasios D. Panagopoulos (thpanag@ece.ntua.gr).
The authors are with the School of Electrical and Computer Engineering, National Technical University of Athens, Greece.

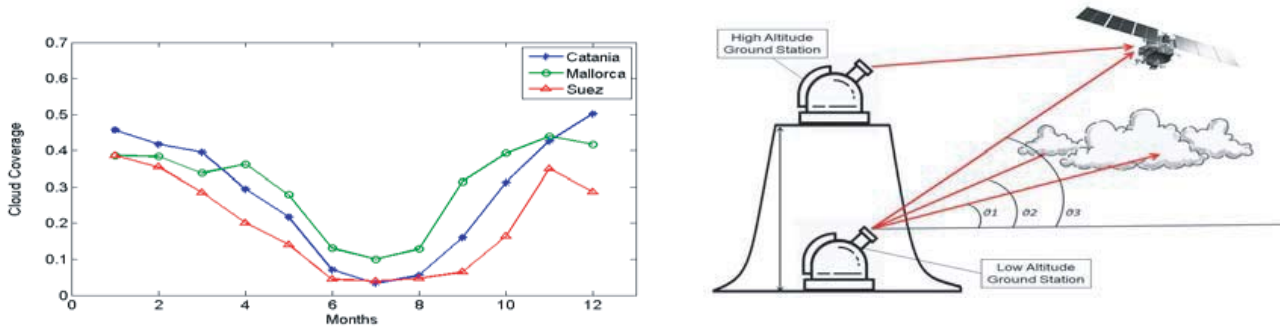

(a) (b)

Figure 1. (a) Monthly variation of cloud coverage. (b) Optical satellite link — CFLOS (elev. angle, high altitude).

In this letter, a monthly CFLOS time series generator for single and multiple links (spatial diversity) is proposed. The proposed generator uses monthly ILWC statistical parameters and captures the monthly variability of cloud coverage. Additionally the new methodology takes into account the temporal and spatial correlation of ILWC along the slant path and captures the variability of CFLOS probability with the elevation angle of the slant path link and the altitude of the stations. The monthly synthesizer is an extension of the model presented in [5] and takes advantage of the use of stochastic differential equations for the generation of monthly ILWC temporally and spatially correlated time series. In contrast with [5] where annual statistics are used and only the single slant path is modeled, in this contribution a) the monthly variability of cloud coverage is captured, b) the mathematical framework for the generation of time series correlated on temporal and spatial domain for spatial diversity scenario (multiple optical links) taking into account the spatial correlation of clouds between the different locations is firstly proposed.

The remainder of the paper is structured as follows: in Section 2 the proposed monthly CFLOS synthesizer is presented. In Section 3 single and joint CFLOS numerical results are presented using the proposed methodology and assuming a GEO satellite. Finally in Section 4 some conclusions are drawn.

2. MONTHLY CFLOS TIME SERIES GENERATOR

The geometrical configuration of single optical link is shown in Fig. 1(b). In this Section, the methodology proposed in [5] is extended in order to develop a monthly CFLOS time series generator for multiple links. In optical satellite communications an on/off channel with the cloud occurrence is assumed. To this end, CFLOS probability is defined as $P_{\text{CFLOS}} = 1 - P_{\text{CLW}}$ where P_{CLW} is the probability of ILWC > 0 and as a result the probability of cloud coverage. In order to incorporate the effect of clouds in the optical link, 3D cloud fields, correlated in space, and time for each place of interest, where optical ground stations (OGS) are located, are generated. The cloud fields are created using monthly statistical parameters of ILWC. Firstly for each OGS, a 2-D ILWC map which consists of several ILWC grids with spatial resolution of $1\,\text{km} \times 1\,\text{km}$ is generated. Such a map is synthesized for each OGS for each month. It is assumed that ILWC is constant within a grid of $1\,\text{km} \times 1\,\text{km}$. The ILWC map for a station can be mathematically described as $L^m_{\text{map, OGS}} = [L^m_1, L^m_2, ..., L^m_n]$ where $m = 1...12$ are the months starting from January up to December; L^m_i are the ILWC grids along the slant path for every month; and n is the number of grids along the whole slant. An example of an ILWC map for a specific month is illustrated in Fig. 2.

For the evaluation of the site diversity technique for each OGS, a different ILWC map is generated. These maps are also correlated both in temporal and in spatial domains to each other. The total ILWC field for multiple stations, where ILWC maps for different stations are incorporated, can be expressed as $L^m_{\text{total\_field}} = [L^m_{\text{map, OGS\_1}}, L^m_{\text{map, OGS\_2}}, ..., L^m_{\text{map, OGS\_}k}]$. For the generation of L^m_i, the following expression

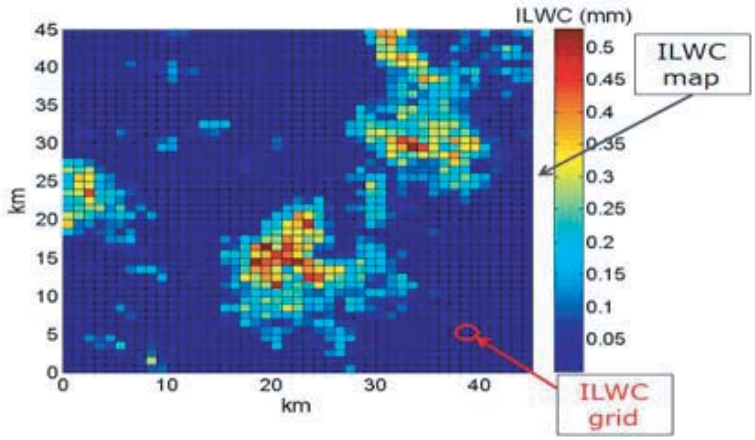

Figure 2. 2D ILWC map snapshot.

is employed:

$$L_i^m(t) = \left\{ \begin{array}{ll} \exp\left[Q^{-1}\left(\frac{1}{P_{\mathrm{CLW},i}^m} Q\left(G_i(t)\right)\right) \times \sigma_i^m + \mu_i^m\right] & G_i(t) \geq \alpha_{th,i}^m \\ 0 & G_i(t) \leq \alpha_{th,i}^m \end{array} \right\} \tag{1}$$

where μ_i^m, σ_i^m, and $P_{\mathrm{CLW},i}^m$ are the mean value standard, deviation, and probability of cloud coverage (ILWC > 0) of $ln(L)$ for each month for each grid. For an OGS, it is assumed that the statistical parameters of $ln(L)$ are constant (i.e., the same) for all the grids along the slant path. Different stations have different statistical parameters. Therefore, for each location of interest, for each month, following the regression fitting methodology presented in [7], the monthly statistical parameters can be derived from ERA-Interim database. Moreover, $Q(\,)$ is the Gaussian Q-function, and $\alpha_{th,i}^m$ threshold is calculated through $a_{th} = Q^{-1}(P_{\mathrm{CLW}})$. $G_i(t)$ is the Gaussian process for the generation of each grid. $G_i(t)$ can be defined as the superposition of two Gaussian processes $X_i^1(t), X_i^2(t)$ as $G_i(t) = \gamma_1 X_i^1(t) + \gamma_2 X_i^2(t)\,(i = 1...n * k)$ where γ_1, γ_2 are extracted from [9]. The Gaussian processes $X_i^g(t)$, $(g = 1, 2)$ are generated using the solution of the n-dimensional Stochastic Differential Equation:

$$\mathbf{X}_{i,t}^g = e^{t\cdot\mathbf{B}^g} \cdot \mathbf{X}_0^k + e^{t\cdot\mathbf{B}^g} \cdot \int_0^t e^{-s\cdot\mathbf{B}^g} \cdot \mathbf{S}^g \cdot d\mathbf{W}_s, \;\; (g = 1,\, 2) \tag{2}$$

where $\mathbf{B}^g$ is the diagonal matrix $\mathbf{B}^g = [b_{ij}^g]_{1\leq i,\, j\leq n*k}$ with $b_{ij}^g = -\beta^g \cdot \delta_{ij}$ where δ_{ij} is the Kronecker delta function, and β^g are the dynamic parameters of the Gaussian processes of ILWC derived from [9]. In $\mathbf{B}^g$, the temporal correlation of ILWC is captured. $W(t)$ is the $n * k$-dimensional Wiener process $\mathbf{W}(t) = [W_1(t), ..., W_{n*k}(t)]^T$. Finally, $\mathbf{S}^g$ is computed using Cholesky decomposition of $\mathbf{\Lambda}^g = \mathbf{S}^g * (\mathbf{S}^g)^T$ where $\mathbf{\Lambda}^g = 2 * \beta^g * \mathbf{C}$, and $\mathbf{C}$ is the spatial correlation matrix of $L_{\mathrm{total\_field}}$.

$$\mathbf{C} = \begin{bmatrix} 1 & . & . & . & \rho_{1,\,n*k} \\ . & 1 & & & . \\ . & & 1 & & . \\ . & & & 1 & . \\ \rho_{n*k,1} & . & . & . & 1 \end{bmatrix} \tag{3}$$

ρ is the correlation of the Gaussian process estimated using the expression proposed in [8]. ρ depends on the separation distance of the grids. For different stations, this distance is based on the separation distance of the OGS. In really large separation distances (more than 500 km), correlation factor ρ takes values lower than 0.1. Therefore, following the proposed procedure all the elements of $L_{\mathrm{total\_field}}^m$ are temporally and spatially correlated.

In order to develop a 3D cloud monthly generator, the vertical extent of ILWC is employed, and then the 2D ILWC maps are converted into 3D maps. In [8], the vertical profile of liquid water content

of a grid of 1 km × 1 km is estimated using the following expression:

$$\tilde{w}_i^m(h,t) = \begin{cases} \frac{L_i^m(t)}{c_i^2(t)^{c_i^1(t)}\Gamma(c_i^1(t))}(h-h_0)^{c_i^1(t)-1}\, e^{-(h-h_0)/c_i^2(t)} & \text{for } h \geq h_0 \\ 0 & \text{for } h < h_0 \end{cases} \tag{4}$$

$$c_i^1(t) = 4.27e^{-4.93(L_i^m(t)+0.06)} + 54.12e^{-61.25(L_i^m(t)+0.06)} + 1.71$$

$$c_i^2(t) = 3.17c_i^1(t)^{-3.04} + 0.074$$

This expression depends on the ILWC and height among others. $w_i^m(h,t)$ in g/m^3 is the Liquid Water Content depending on the vertical height; h in km is the vertical height of cloud; $\Gamma(\,)$ is the Gamma function; $L_i^m(t)$ are the ILWC time series generated according to expression (1); and h_0 is the cloud base height that is derived from the statistical distribution [8] or from available statistics for a specific location if they are available. In this analysis, the statistical distribution of [8] is used. Now, in order to estimate the vertical extent of cloud fields, the top height is needed since the cloud base height is taken from the distribution of [8]. In order to compute the cloud top height based on the remark of [8], Equation (4) is solved as $\tilde{w}_i^m(h,t) \to 0$ for $\tilde{w}_i^m(h,t) \leq 0.06 \cdot L_i^m(t)$. Since each grid has dimensions of 1 km and 1 km on x, y axes, respectively, and the vertical extent of each grid of each map is computed, the 3D configuration of ILWC along the whole slant path for each month is defined. Therefore, CFLOS along the slant path can be computed taking into account the elevation angle and altitude of each OGS. For each OGS it is assumed that if there is at least one cloud grid (grid with ILWC > 0) along the slant path that intersects with the link, then the whole optical slant path is considered blocked. Thus, for each station concurrent, monthly CFLOS time series are generated. CFLOS time series are temporally and spatially correlated. For multiple OGSs (OGSN), if at least one OGS is not blocked by clouds, then the OGSN is considered free of clouds, and the monthly joint CFLOS statistics are calculated. In

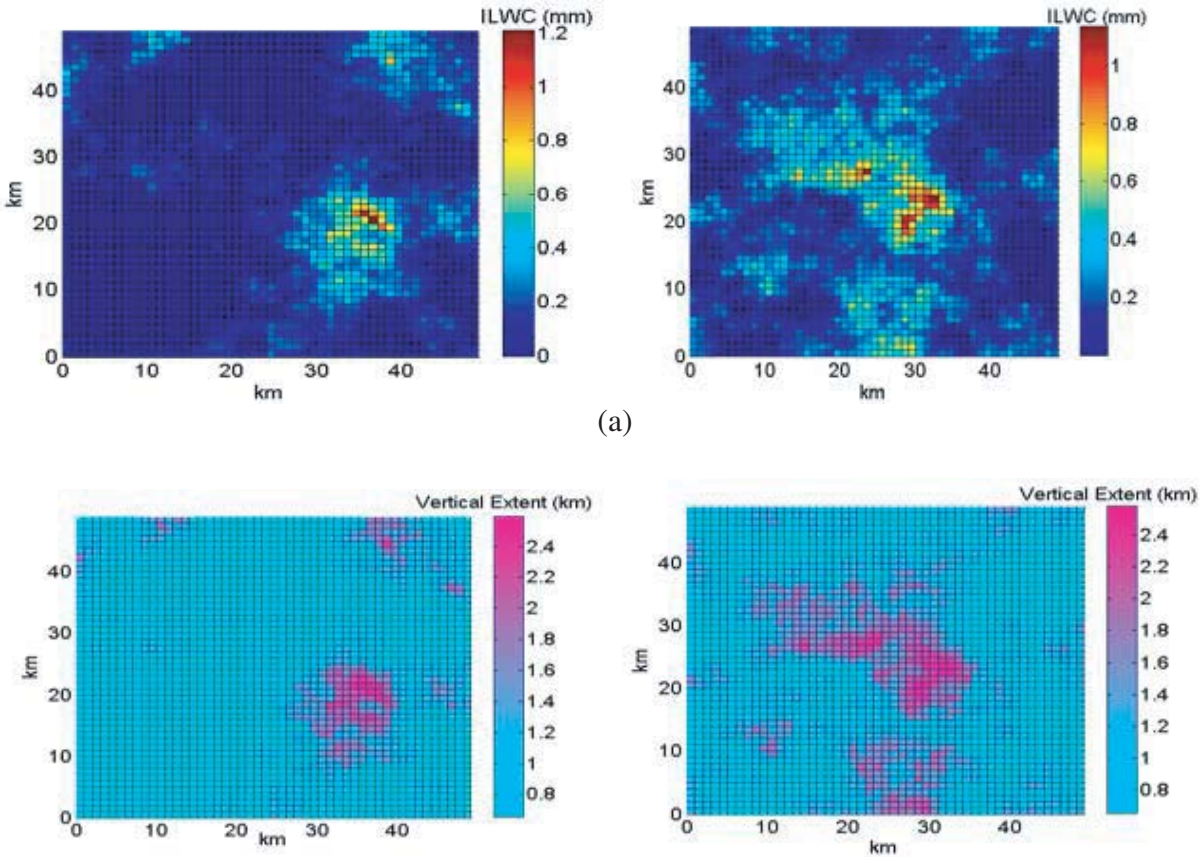

(a)

(b)

Figure 3. (a) 2D ILWC maps. (b) 3D maps — vertical extent.

Figure 3, snapshots of 2D ILWC maps (up) and 3D maps (down) correlated on spatial and temporal domain for a hypothetical OGS are presented. The left ones are at time $t = t_0$ while the right ones are 60 min later. From these figures the temporal and spatial variability of clouds and the vertical extent of clouds for a plane of 50×50 km are identified.

3. VALIDATION & SIMULATION RESULTS

The synthesizer proposed in the previous Section is employed for the generation of monthly single and joint CFLOS statistics for a GEO link scenario. Firstly the capability of 2D ILWC monthly synthesizer to reproduce the monthly first order statistics (exceedance probability) of ILWC is identified. ILWC can be described by lognormal distribution [7, 10, 11]. The statistical parameters have been derived from the monthly database of Era-Interim for the period from 1/1/2012 until 31/12/2015. In Figure 4(a) the theoretical and synthesized CCDFs for two months for Catania Italy are reported. It can be observed that the CCDFs derived from the synthesized data and the theoretical ones absolutely coincide. In Figure 4(b) by employing the monthly CFLOS synthesizer, a snapshot of CFLOS time series for a station in Athens, Greece is presented. In this Figure 4(b), one means that the link is not blocked and zero that the link is blocked.

Finally, the proposed synthesizer is employed in order to calculate the monthly CFLOS probability for various locations. The results are given in Table 1. The ILWC statistical parameters used have been derived from the monthly database of Era-Interim for the period from 1/1/2012 until 31/12/2015. The ASTRA 2b GEO satellite at 23.5 deg East is assumed as space segment. For all the locations, the corresponding elevation angles are also tabulated.

It must be noted that the mean annual CFLOS probability for the high altitude station of Tenerife is estimated close to 82.8% which is in line with the results in [4] where cloud mask statistics with 5×5 spatial resolutions is used. If the altitude is not incorporated in the CFLOS probability calculation and using the corresponding vertical link the CFLOS is estimated as 55.43%.

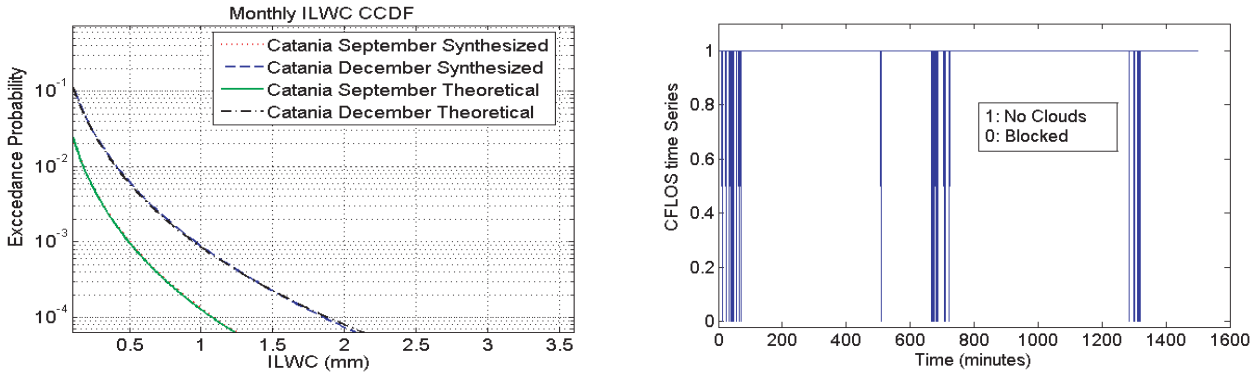

(a) (b)

Figure 4. (a) First order statistics validation of ILWC. (b) CFLOS time series snapshot.

Table 1. Monthly CFLOS statistics.

#	Location	Lat./Lon. (deg)	Alt. (km)	Elev. (deg)	P_{CFLOS}(%) Months: 1–3	P_{CFLOS}(%) Months: 4–6	P_{CFLOS}(%) Months: 7–9	P_{CFLOS}(%) Months: 10–12
1	Tenerife, SP	28.76/−17.89	2.4	33.9	81.8/80.6/81.7	82.9/80/81	85.2/87/87.2	84.6/79/82.3
2	Skinakas, GR	35.12/24.53	1.7	49.1	58.9/63.9/75.3	78.2/84/93.4	98.7/99/91.6	78.5/67/57
3	Catania, It	36.14/24.53	0.2	47	54.3/58.2/60.5	70.6/78.3/92.9	96.6/94.5/84	68.8/57.4/49.9
4	Mallorca, SP	39.6/2.68	0.1	39.4	61.4/61.6/66.2	63.8/72.1/87	90/87.1/68.6	61/56/58.3
5	Madrid, SP	40.43/−4.25	0.8	35.3	54/53.2/53	49/65/76	88.4/87/69	55/52/50.6
6	Nice, FR	43.7/7.3	0.3	37	53.3/54/58	60/65/78.6	86.6/84.8/70	55.8/50.3/56
7	Suez, EG	30/32.5	0.15	53.7	72.2/71.1/79	87.5/89.4/97.9	97.6/97.9/94.3	88/72/75.6
8	Dubai, UAE	25.12/55.6	0.16	43.8	86.3/88.5/81.4	79.6/91.5/96.7	86.7/87.5/92.9	96.5/88.8/86.9
9	Doha, Qatar	25.32/55.6	0.13	47.3	84.9/84.7/76.7	77.7/89.7/98.8	92.8/93.8/98.8	95.5/84.2/82.9

Table 2. Joint monthly CFLOS statistics.

Stations	Joint $P_{\mathrm{CFLOS}}(\%)$ Months: 1–3	Joint $P_{\mathrm{CFLOS}}(\%)$ Months: 4–6	Joint $P_{\mathrm{CFLOS}}(\%)$ Months: 7–9	Joint $P_{\mathrm{CFLOS}}(\%)$ Months: 10–12
{8}	86.3/88.5/81.4	79.6/91.59/6.7	86.7/87.5/92.9	96.5/88.8/86.9
{8}, {9}	97.5/97.8/94.9	94.7/98.9/99.9	98.76/99/98.9	99.8/97.8/97.2
{8}, {9}, {7}	99.3/99.37/98.9	99.3/99.9/99.9	99.9/99.9/99.9	99.9/99.4/99.3
{8}, {9}, {7}, {1}	99.9/99.9/99.8	99.9/99.9/99.9	99.9/99.9/99.9	99.9/99.9/99.9
{8}, {9}, {7}, {1}, {2}	99.9/99.9/99.9	99.9/99.9/99.9	99.9/99.9/99.9	99.9/99.9/99.9

Finally, in Table 2 joint monthly CFLOS statistics are reported using the multidimensional space time monthly synthesizer for the 5 stations with the highest mean CFLOS, meaning that the stations $\{8\},\{9\},\{7\},\{1\}$, and $\{2\}$ of Table 1 are used. In the first row of Table 2, the monthly CFLOS of station $\{8\}$ is exhibited in the second row the joint monthly CFLOS of stations $\{8\},\{9\}$, in third row the joint CFLOS of $\{8\},\{9\},\{7\}$, etc. Using these locations, the availability for the whole OGSN of more than 99.9% for each month can be achieved. In the presented results in Table 2, we give the achieved threshold of 99.9%.

4. CONCLUSIONS

In this letter, an accurate monthly time series synthesizer for the derivation of the monthly CFLOS is presented. The proposed synthesizer takes into account the spatial and temporal variability of clouds and takes as inputs the monthly statistical parameters of ILWC the elevation angle of the link and the altitude of the station for high altitude stations. Moreover, monthly joint CFLOS statistics are presented. The proposed monthly CFLOS synthesizer can be used for the optimum design of an OGSN regarding the number of ground terminals and the achieved availability.

REFERENCES

1. Kaushal, H. and G. Kaddoum, "Optical communication in space: Challenges and mitigation techniques," *IEEE Comm. Surv. & Tut.*, Vol. 19, No. 1, 57–96, Aug. 2016.
2. Fuchs, C. and F. Moll, "Ground station network optimization for space-to ground optical communication links," *IEEE/OSA J. of Opt. Comm. and Net.*, Vol. 7, No. 12, 1148–1159, Dec. 2015.
3. Poulenard, S., et al., "Ground segment design for broadband geostationary satellite with optical feeder link," *J. Opt. Commun. Netw.*, Vol. 7, No. 4, 325–336, 2015.
4. Fuchs, C., et al., "Performance estimation of optical LEO downlinks," *IEEE Journal on Selected Areas in Communications*, Vol. 36, No. 5, 1074–1085, May 2018.
5. Lyras, N. K., et al., "Cloud attenuation statistics prediction from Ka-band to optical frequencies: Integrated liquid water content field synthesizer," *IEEE Transactions on Antennas and Propagation*, Vol. 65, No. 1, 319–328, Jan. 2017.
6. Lyras, N. K., et al., "Cloud free line of sight prediction modeling for optical satellite communication networks," *IEEE Communications Letters*, Vol. 21, No. 7, 1537–1540, Jul. 2017.
7. Lyras, N. K., et al., "Optimum monthly based selection of ground stations for optical satellite networks," *IEEE Communications Letters*, Vol. 22, No. 6, 1192–1195, Jun. 2018.
8. Luini, L. and C. Capsoni, "Modeling high-resolution 3-D cloud fields for earth-space communication systems," *IEEE Transactions on Antennas and Propagation*, Vol. 62, No. 10, 5190–5199, Oct. 2014.
9. ITU-R Recommendation P.1853-1, "Tropospheric attenuation time series synthesis," ITU-R P.1853-1, Geneva, Switzerland, 2012.
10. ITU-R Recommendation P.840-6, "Attenuation due to clouds and fog," Geneva, Switzerland, 2013.
11. Perlot, N., T. Dreischer, C. M. Weinert, and J. Perdigues, "Optical GEO feeder link design," *Proc. Future Netw. Mobile Summit (FutureNetw)*, 1–8, Jul. 2012.